Proceedings of the Estonian Academy of Sciences,
2015, **64**, 3, 219–225
doi: 10.3176/proc.2015.3.03
Available online at www.eap.ee/proceedings

MECHANICS

Elastic pantographic 2D lattices: a numerical analysis on the static response and wave propagation

Francesco dell'Isola[a,b*], Ivan Giorgio[a,b], and Ugo Andreaus[a]

[a] Department of Structural and Geotechnical Engineering, Sapienza University of Rome, 18 Via Eudossiana, 00185 Roma, Italy
[b] MeMoCS, International Research Center for the Mathematics & Mechanics of Complex Systems, Università dell'Aquila, Via Giovanni di Vincenzo 16/3, 67100 L'Aquila, Italy

Received 11 December 2014, accepted 7 May 2015, available online 20 August 2015

Abstract. In the present paper we consider a structure constituted by 'long' Euler beams forming two mutually intersecting arrays and interacting via internal pivots, which we call pantographic 2D lattices. For this structure, small deformations, but possibly large displacements, can be considered. We performed numerical simulations concerning 2D pantographic sheets of rectangular shape with two families of beam arrays cutting at 90 degrees. The set of theoretical tools needed to describe the continuous limit for such kind of structures goes beyond classical continuum mechanics. In particular, non-Cauchy contact actions can arise in the considered context. The results motivate further investigations, the first step reasonably being the determination of a generalized continuum model.

Key words: higher order continua, fabrics, textiles, finite element analysis, wave propagation.

1. INTRODUCTION

It is commonly accepted in continuum mechanics that mechanical interactions are due to surface contact forces, these interaction forces being represented by the stress tensor σ (Cauchy Theorem). As it is well known, when dealing with the equilibrium of elastic media, this description can easily be recovered through variational considerations. These classical conclusions, however, are valid in the context of first gradient Cauchy continua, but cease to hold when more peculiar structures are considered. Specifically, discrete systems leading in the homogenized limit to higher order continua may provide relatively simple examples, and thus a better understanding, of these new mechanical interactions. The literature concerning higher order continua is of course very wide; for some works presenting relations with homogenization problems, the reader can see e.g. [10,16,31,32,38,39]. The theory of micromorphic media, which can be viewed as a generalization of higher gradient continua, can also offer tools useful to deal with homogenization processes (see e.g. [15,25,29]). The behaviours that can be shown in this kind of context are very rich, entailing, for instance, the possibility of phase transitions (see e.g. [1,11,12,33,40]) and instabilities of the type presented e.g. in [20–23,30]).

Herein we consider a structure constituted by suitably long Euler beams. The simple Euler model for the beam still represents the basis for interesting scientific subjects in the case of peculiar geometrical or elastic characteristics (see e.g. [2,6]). In the structure considered in our model, the beams form parallel and orthogonal arrays. Each beam belonging to an array is interconnected via internal pivots to all the beams of the other array. We call the resulting structure a pantographic 2D lattice. This system is characterized by three scales of different length: the diameter of the beams (on which of course the stiffness depends), the spacing between the beams, and the distance between the closest pivots. As a concrete example from the 'real world', one can consider the Kevlar fibres shown in Fig. 1a.

The aim of the present paper is to introduce a model based on the considered structure and characterized by very simple kinematics, and briefly discuss, by means of some numerical simulations, its basic characteristics.

* Corresponding author, francesco.dellisola@uniroma1.it

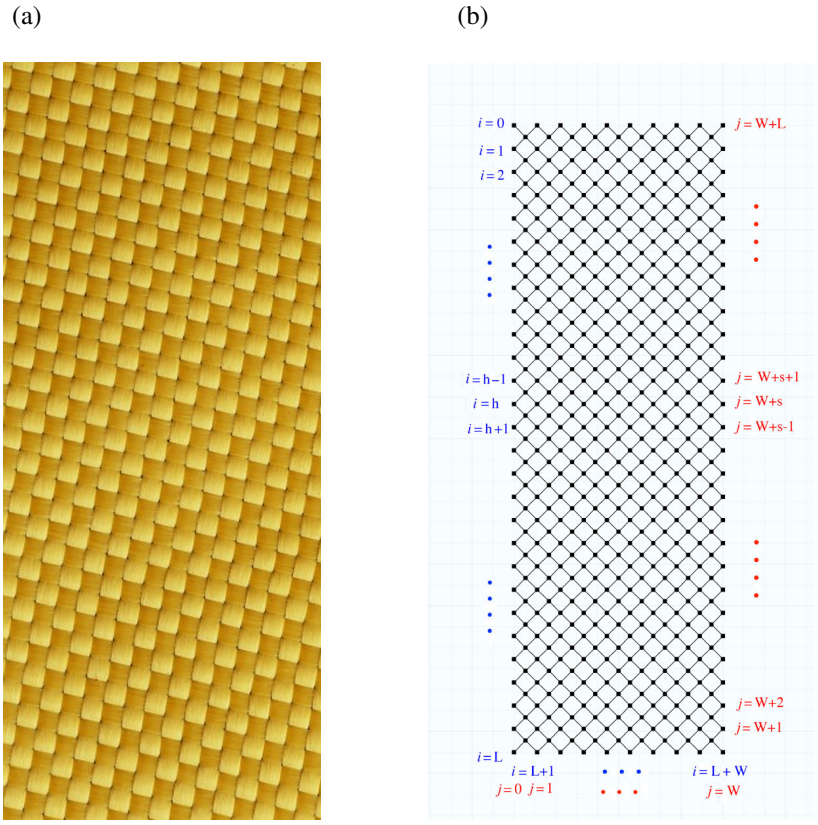

Fig. 1. Photo of Kevlar fibres (a) and the reference configuration (b).

2. THE MODEL

The reference configuration C^* for our mechanical model is graphically represented in Fig. 1b. Lines indicate beams, which are divided in two families, α and β, of parallel and equally spaced beams (at the distance d), reciprocally orthogonal in C^*. The beams are arranged in a rectangle (sized $\sqrt{2}\mathrm{L}d \times \sqrt{2}\mathrm{W}d$ in C^*; where L and W are integers representing the number of intervals between the beams along the height (h) and the width (l)) whose sides are crossed by α and β at 45 degrees in C^*. We indicate the beams belonging to α and β, respectively, with integer indexes i and j ranging from 0 to $\mathrm{L}+\mathrm{W}$, where the extreme values indicate points representing 'degenerate' beams. Referring to Fig. 1b, we start counting from the upper left corner for the family α and from the lower left corner for the family β. In this way every intersection is uniquely determined by two integers (i, j) indicating the two beams to which the intersection belongs.

Each beam has a standard linearized Euler strain energy density given by

$$\mathscr{E} = \frac{k_M(u'')^2 + k_N(w')^2}{2}. \qquad (1)$$

Here u and w are respectively the values of transverse and axial displacements $\mathbf{u}$ and $\mathbf{w}$ with respect to C^*, and k_M and k_N are respectively bending and axial stiffness coefficients, which in the real object depend of course on the diameter of the beams.

The dots in Fig. 1a represent hinges whose kinematics are defined by

$$\mathbf{u}_b(i,j) + \mathbf{w}_b(i,j) = \mathbf{u}_c(i,j) + \mathbf{w}_c(i,j), \qquad (2)$$

which must hold for $\forall b \in \alpha, c \in \beta$ and for all integers i, j such that $0 \le i \le \mathrm{L}+\mathrm{W}$ and $0 \le j \le \mathrm{L}+\mathrm{W}$.

Informally speaking, the actual configuration C^t is then characterized, with respect to C^*, by a 'large' displacement due to the contribution of rigid rotations allowed by the hinges – which do not interrupt the continuity of beams – and 'small' displacements due to axial and bending elastic deformations.

3. NUMERICAL RESULTS AND DISCUSSION

Numerical simulations for textile composites have of course already been considered in the literature (see e.g. [27,28]). For our numerical simulations, we chose the value 0.1 m for the length of the lower side of the rectangle, and a height h whose value is given for every single simulation. As we had the already mentioned Kevlar fibres [3] in mind as a reference model, we chose

the values 1.96×10^{-2} N m^2 and 7.85×10^4 N for k_M and k_N, corresponding to a beam with an elliptic section of semiaxes $a = 0.001$ m and $b = 0.00025$ m (area $A = 7.85 \times 10^{-7}$ m^2, inertia moment of the cross-section around its minor axis $J = 1.96 \times 10^{-13}$ m^4) rotating around the minor one. To conclude our geometry, we selected $d = 0.0(1)$ m for the static simulations and $d = 0.00(5)$ m for the dynamic ones.

The mechanical parameters were again selected referring to the Kevlar fibres described in [3]. Therefore we set the mass density $\rho = 1450$ kg/m^3, $Y = 100$ GPa for Young's modulus, and $\nu = 0.2$ for Poisson's ratio. The material was assumed to be linearly elastic.

Numerical computation in discrete systems can very easily lead to delicate numerical problems. A set of tools that are useful when dealing with peculiar geometrical configurations, like those considered in our model, are exposed in [7–9,14,17–19,37].

All numerical simulations were performed with *COMSOL Multiphysics*®.

3.1. Statics

We started considering static simulations in which the system is deformed by means of imposed displacements applied to the 10 points belonging to the upper side. The displacement is parallel to the height of the rectangle and has the value $u_\Delta = \frac{h}{3}$. The displacement parallel to the upper side is equal to zero, and the points belonging to the lower side are built in. In this simulation we chose $h = 0.3$ m.

The deformed shapes of the system in the given conditions are shown in Fig. 2. In Fig. 2a the deformation field of the beam axes for α and β is also plotted, while in Fig. 2b the maximum and minimum values for the axial strain due to bending are plotted. In both panels the upper and lower sides are of course undeformed, and the maximum striction is observed around the centre. One can observe that, as it is well known in the continuous case, the two triangular regions having the upper and lower sides as the basis are stressed at a very low level, while a higher concentration of stress is observed in the vertexes, and the stress gradually decreases along the sides of the two aforementioned triangular regions.

The global elongation along the height is, as we set, 1/3, while locally one can measure a maximum axial strain due to the axial force $\approx 7 \times 10^{-3}$ and a maximum axial strain due to the bending moment $\approx 3 \times 10^{-2}$. Therefore, as already observed, we have here small strains and clearly large displacements and rotations.

All the maximum values for stresses and deformations are well below the yielding values characterizing the material (Kevlar) we chose as a reference in this paper.

3.2. Parametric analysis

In this section we begin considering the dynamics of our system. Specifically, we impose a time-dependent displacement, oriented along the direction of α, on the points belonging to the upper side, the lower side being, as before, built in. The displacement has an impulse-like character, i.e. it is sharp and concentrated in a short interval around $t = 0.005$ s, vanishing elsewhere. It is analytically represented by the function $\mathfrak{I}(\mathrm{t}) = u_0 * \mathrm{sech}[\tau(t - t_0)]$, where $u_0 = 0.05$ m and $t_0 = 0.005$ s, and τ is a parameter affecting the duration of the impulse.

We provide here (Fig. 3) a parametric analysis concerning the effect of changing τ while keeping all other parameters unchanged. The height h of the rectangle is set to 2.5 m, and for τ the values (from left to right) 1500, 2500, and 3500 s^{-1} are considered; the plots refer to the situation at $t = 0.01$ s. In Fig. 3 (as well as in Figs 4 and 5) the absolute value of the rotations of the cross-sections is plotted by means of colour maps.

Observing the length of the perturbed zone, one can conjecture a significant dispersion in wave propagation, whose level appears to be positively influenced by an increase in τ. Dispersion in such kind of discrete elastic media was already proven in a one-dimensional context, e.g. in [36], where the case with dispersion is obtained by suitably adjusting the parameters characterizing the system (we will observe in more detail the dispersion in the following section). As it is visible from the length of the unperturbed zone close to the upper side, the velocity of the waves is also positively influenced by the values of τ.

Another parametric study involved the intensity of the impulse, controlled by varying u_0. In Fig. 4 the values (from left to right) $\frac{0.05}{\sqrt{2}}$, 0.05, and $0.05\sqrt{2}$ are employed. In this case, both the velocity and the dispersion are unchanged, and only the higher deformations due to higher intensities are observed.

3.3. Dynamics

In the last simulation, plotted in Fig. 5, we considered the propagation of a wave in our medium. Wave propagation has been considered, of course, in an enormously rich class of contexts in the literature; in particular, cases which present analogies with our discrete model have been studied (see e.g. [24,34,35]), and even some cases of very interesting exotic behaviours were observed (see [13,26,41]).

In our simulation, we imposed a time-dependent displacement – analytically given by the aforementioned function $\mathfrak{I}(\mathrm{t})$ – oriented along the height of the rectangle and applied to the points belonging to the upper side. The height h is set to 2.5 m, and on the horizontal axis, the time relative to every snapshot is given. In this dynamic simulation, an X-shaped wave front is visible, and a more appropriate assessment of dispersion is possible, as the length of the perturbed zone is clearly increasing in time. The last two snapshots also show the reflection of the wave on the lower side (which, we recall, is built in).

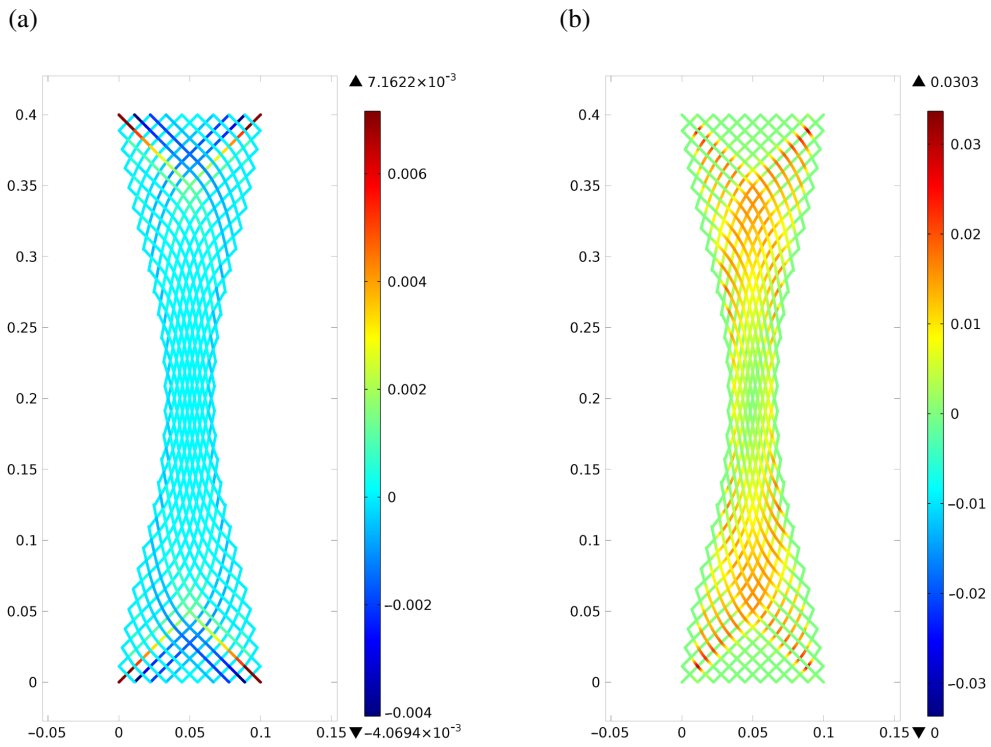

Fig. 2. Axial strain due to the axial force (a) and the bending moment (b).

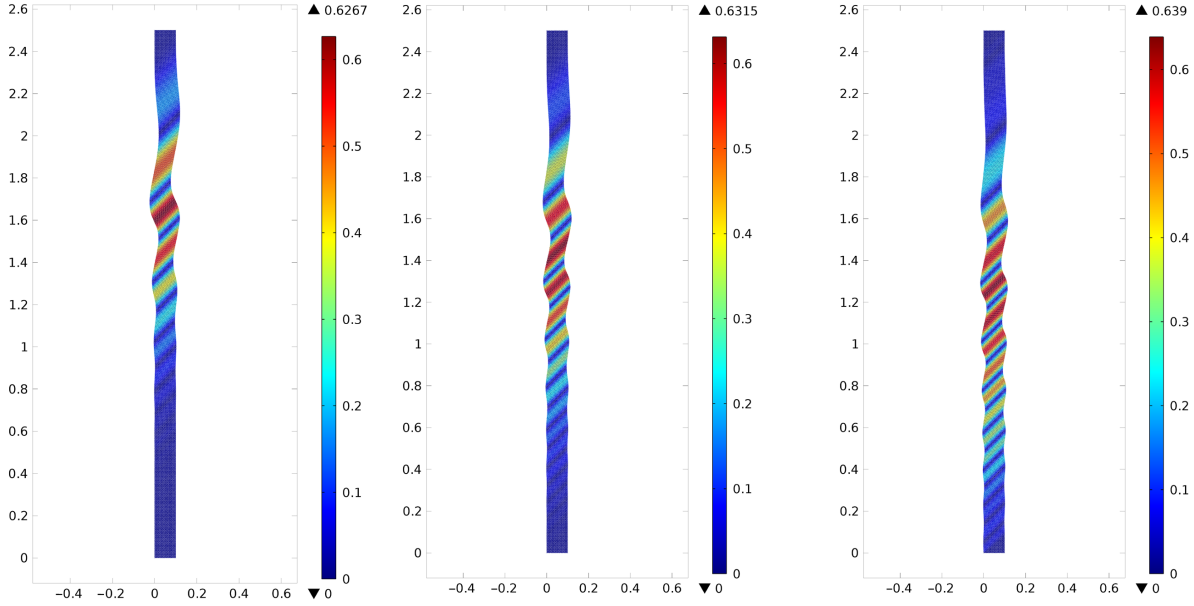

Fig. 3. Parametric study on the duration of the impulse.

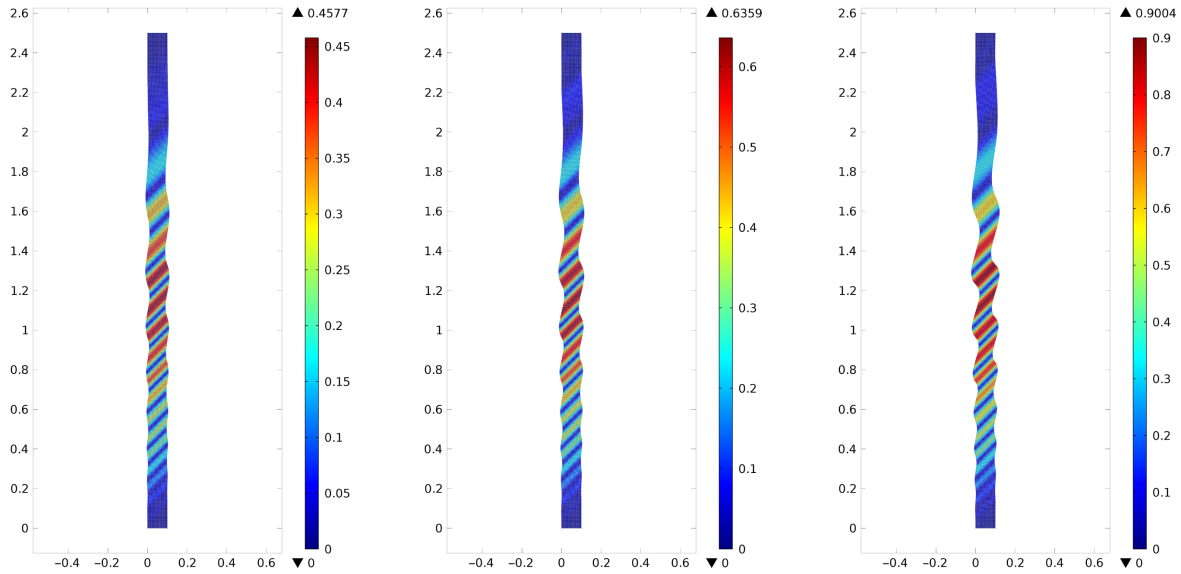

Fig. 4. Parametric study on the intensity of the impulse.

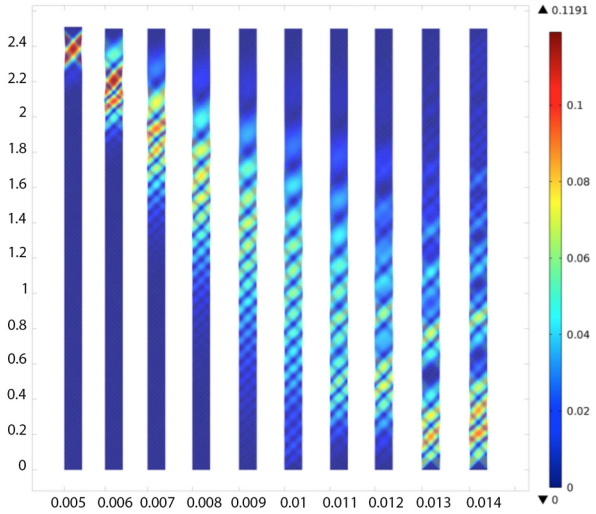

Fig. 5. Wave propagation after an imposed displacement on the upper side.

4. CONCLUSIONS

The main aim of the paper was to introduce a simple model for a pantographic 2D lattice, which can have, in its homogenized limit, very interesting properties as a continuum medium. The model can be enriched, of course, by introducing geometrical non-linearities or considering dissipation phenomena [4,5] in order to improve the accuracy in describing real objects. The theoretical interest, moreover, is also connected to a set of possible practical applications to different fields. In this connection, we can mention three main areas for which realistic applications of the considered structures are predictable: (i) vascular prostheses, due to the required properties of anisotropy and selective penetrability; (ii) aeronautic, aerospace, and naval engineering, due to the potential lightness of the resulting components; and (iii) acoustic filters, due to the possibility of finding suitable inclusions that can damp selected frequencies. Therefore, further investigation on the considered pantographic structures looks both promising and potentially very rich in scientific content.

REFERENCES

1. Altenbach, H. and Eremeyev, V. A. Analysis of the viscoelastic behavior of plates made of functionally graded materials. *Z. angew. Math. Mech.*, 2008, **88**(5), 332–341.
2. Bîrsan, M., Altenbach, H., Sadowski, T., Eremeyev, V. A., and Pietras, D. Deformation analysis of functionally graded beams by the direct approach. *Compos. Part B-Eng.*, 2012, **43**(3), 1315–1328.
3. Cao, J., Akkerman, R., Boisse, P., Chen, J., Cheng, H. S., de Graaf, E. F. et al. Characterization of mechanical behavior of woven fabrics: experimental methods and benchmark results. *Compos. Part A-Appl.S.*, 2008, **39**(6), 1037–1053.
4. Carcaterra, A. and Akay. A. Dissipation in a finite-size bath. *Phys. Rev. E*, 2011, **84**, 011121.
5. Carcaterra, A., Roveri, N., and Pepe, G. Fractional dissipation generated by hidden wave-fields. *Math. Mech. Solids*, 2014. doi: 10.1177/1081286513518941.
6. Cazzani, A. On the dynamics of a beam partially supported by an elastic foundation: an exact solution-set. *Int. J. Str. Stab. Dyn.*, 2013, **13**(08), 1350045.
7. Cazzani, A. and Ruge, P. Numerical aspects of coupling strongly frequency-dependent soil-foundation models with structural finite elements in the time-domain. *Soil Dyn. Earthq. Eng.*, 2012, **37**, 56–72.
8. Cazzani, A., Malagù, M., and Turco, E. Isogeometric analysis of plane-curved beams. *Math. Mech. Solids*, 2014. doi: 10.1177/1081286514531265.
9. Cuomo, M., Contrafatto, L., and Greco, L. A variational model based on isogeometric interpolation for the analysis of cracked bodies. *Int. J. Eng. Sci.*, 2014, **80**, 173–188.
10. Dos Reis, F. and Ganghoffer, J. F. Equivalent mechanical properties of auxetic lattices from discrete homogenization. *Comput. Mater. Sci.*, 2012, **51**, 314–321.
11. Eremeyev, V. A. and Pietraszkiewicz, W. Phase transitions in thermoelastic and thermoviscoelastic shells. *Arch. Mech.*, 2009, **61**(1), 41–67.
12. Eremeyev, V. A. and Zubov, L. M. On the stability of equilibrium of nonlinear elastic bodies with phase transformations. *Proc. USSR Acad. Sci. Mech. Solids*, 1991, **2**, 56–65.
13. Fornberg, B. *A Practical Guide to Pseudospectral Methods*. Cambridge University Press, Cambridge, 1998.
14. Garusi, E., Tralli, A., and Cazzani, A. An unsymmetric stress formulation for Reissner–Mindlin plates: a simple and locking-free rectangular element. *Int. J. Comp. Eng. Sci.*, 2004, **5**(3), 589–618.
15. Ghiba, I. D., Neff, P., Madeo, A., Placidi, L., and Rosi, G. The relaxed linear micromorphic continuum: existence, uniqueness and continuous dependence in dynamics. *Math. Mech. Solids*, 2014. doi: 1081286513516972.
16. Goda, I., Assidi, M., Belouettar, S., and Ganghoffer, J. F. A micropolar anisotropic constitutive model of cancellous bone from discrete homogenization. *J. Mech. Behav. Biomed. Mater.*, 2012, **16**, 87–108.
17. Greco, L. and Cuomo, M. B-Spline interpolation of Kirchhoff–Love space rods. *Comput. Methods Appl. Mech. Eng.*, 2013, **256**(0), 251–269.
18. Greco, L. and Cuomo, M. An implicit G1 multi patch B-spline interpolation for Kirchhoff–Love space rod. *Comput. Methods Appl. Mech. Eng.*, 2014, **269**(0), 173–197.
19. Greco, L., Impollonia, N., and Cuomo, M. A procedure for the static analysis of cable structures following elastic catenary theory. *Int. J. Solids Struct.*, 2014, **51**(7), 1521–1533.
20. Luongo, A. and Piccardo, G. Linear instability mechanisms for coupled translational galloping. *J. Sound Vib.*, 2005, **288**(4), 1027–1047.
21. Luongo, A. and Zulli, D. Dynamic instability of inclined cables under combined wind flow and support motion. *Nonlinear Dynam.*, 2012, **67**(1), 71–87.
22. Luongo, A., Paolone, A., and Piccardo, G. Postcritical behavior of cables undergoing two simultaneous galloping modes. *Meccanica*, 1998, **33**(3), 229–242.
23. Luongo, A., Zulli, D., and Piccardo, G. A linear curved-beam model for the analysis of galloping in suspended cables. *J. Mech. Mater. Struct.*, 2007, **2**(4), 675–694.
24. Madeo, A., Neff, P., Ghiba, I. D., Placidi, L., and Rosi, G. Wave propagation in relaxed micromorphic continua: modeling metamaterials with frequency band-gaps. *Continuum Mech. Therm.*, 2013. doi: 10.1007/s00161-013-0329-2.
25. Madeo, A., Neff, P., Ghiba, I. D., Placidi, L., and Rosi, G. Band gaps in the relaxed linear micromorphic continuum. *Z. angew. Math. Mech.*, 2014. doi: 10.1002/zamm.201400036.
26. Maugin, G. A. Solitons in elastic solids (1938–2010). *Mech. Res. Commun.*, 2011, **38**(5), 341–349.
27. Nahine, H. and Boisse, P. Tension locking in finite-element analyses of textile composite reinforcement deformation. *C.R. Acad. Sci., Ser. IIb: Mec., Phys.*, 2013, **341**(6), 508–519.
28. Nahine, H. and Boisse, P. Locking in simulation of composite reinforcement deformations. Analysis and treatment. *Compos. Part A-Appl.S.*, 2013, **53**, 109–117.
29. Neff, P., Ghiba, I.-D., Madeo, A., Placidi, L., and Rosi, G. A unifying perspective: the relaxed linear micromorphic continuum. *Continuum Mech. Therm.*, 2013, **26**(5), 639–681.
30. Piccardo, G., Pagnini, L. C., and Tubino, F. Some research perspectives in galloping phenomena: critical conditions and post-critical behavior. *Continuum Mech. Therm.*, 2014, 5, **27**, 261–285.
31. Pideri, C. and Seppecher, P. A second gradient material resulting from the homogenization of an heterogeneous linear elastic medium. *Continuum Mech. Therm.*, 1997, **9**(5), 241–257.
32. Pideri, C. and Seppecher, P. Asymptotics of a non-planar rod in non-linear elasticity. *Asymptotic Anal.*, 2006, **48**(1–2), 33–54.

33. Pietraszkiewicz, W., Eremeyev, V., and Konopinska, V. Extended non-linear relations of elastic shells undergoing phase transitions. *Z. angew. Math. Mech.*, 2007, **87**(2), 150–159.
34. Salupere, A. The pseudospectral method and discrete spectral analysis. In *Applied Wave Mathematics: Selected Topics in Solids, Fluids, and Mathematical Methods* (Quak, E. and Soomere, T., eds). Springer, Berlin, 2009, 301–333.
35. Sestieri, A. and Carcaterra, A. Space average and wave interference in vibration conductivity. *J. Sound Vib.*, 2003, **263**(3), 475–491.
36. Tarantino, G. Esempi di utilizzo di differenti ambienti di modellizzazione per lo studio delle onde meccaniche. *Quaderni di Ricerca in Didattica (Science)*, 2010, No. 1, G.R.I.M. (Department of Mathematics, University of Palermo, Italy).
37. Turco, E. and Caracciolo, P. Elasto-plastic analysis of Kirchhoff plates by high simplicity finite elements. *Comput. Methods Appl. Mech. Eng.*, 2000, **190**(5–7), 691–706.
38. Yang, Y. and Misra, A. Higher-order stress-strain theory for damage modeling implemented in an element-free Galerkin formulation. *Comput. Model. Eng. Sci.*, 2010, **64**, 1–36.
39. Yang, Y., Ching, W. Y., and Misra, A. Higher-order continuum theory applied to fracture simulation of nano-scale intergranular glassy film. *J. Nanomech. Micromech.*, 2011, **1**, 60–71.
40. Yeremeyev, V. A., Freidin, A. B., and Sharipova, L. L. Non-uniqueness and stability in problems of the equilibrium of elastic two-phase solids. *Dokl. Ross. Akad. Nauk*, 2003, **391**(2), 189–193.
41. Zabusky, N. J. and Kruskal, M. D. Interaction of solitons in a collisionless plasma and the recurrence of initial states. *Phys. Rev. Lett.*, 1965, **15**, 240–243.

Elastne kahemõõtmeline pantograafiline võre: numbriline analüüs staatilisest tagasisidest ja lainelevist

Francesco dell'Isola, Ivan Giorgio ja Ugo Andreaus

On vaadeldud Euleri taladest koosnevat kahemõõtmelist pantograafilist võret, kus on lubatud väikesed deformatsioonid, kuid suured siirded. Eesmärgiks oli koostada homogeniseeritud pidevale keskkonnale vastav mudel ja teostada numbrilised simulatsioonid. Nende käigus selgitati esiteks, millised pikijõud ja paindemomendid tekivad võret moodustavates talades, kui võre on deformeeritud staatiliselt. Teiseks selgitati lainelevi seaduspärasusi vaadeldavas struktuuris. Sel eesmärgil rakendati mõnedesse võrepunktidesse ajas muutuv siirdeväli. Vaadeldava materjali võimalike rakendustena on välja pakutud vaskulaarseid proteese, lennuki- ja kosmosetööstust ning laevaehitust.